



BASIC FEATURES OF THE PREDICTIVE TOOLS OF EARLY WARNING SYSTEMS FOR WATER-RELATED NATURAL HAZARDS: EXAMPLES FOR SHALLOW LANDSLIDES

Roberto Greco¹, Luca Pagano²

¹University of Campania Luigi Vanvitelli, Naples, 80125, Italy

²University of Naples Federico II, Naples, 80125, Italy

Correspondence to: luca.pagano@unina.it

1

2 **ABSTRACT** To manage natural risks, an increasing effort is being put in the development
3 of early warning systems, which rely on prompt forecasting or recognizing of the
4 catastrophic phenomena and temporarily reducing the exposure of people, preventing
5 or limiting victims. Research efforts aimed at the development and implementation of
6 effective EWS should concern, above all, the definition and calibration of the
7 interpretative model. This paper analyses the main features characterizing predictive
8 models working in early warning systems, by discussing their aims, the evolution stage
9 of the phenomenon where they should be incardinated, and their architecture,
10 regardless of the specific application field. With reference to two different phenomena,
11 namely flow-like landslide and earth flows, both characterized by rapid evolution, the
12 paper describes, by means of three examples, some alternative approaches to the
13 development of the predictive tool and to its implementation in an EWS.

14



1. Introduction

Different natural phenomena turning into catastrophes have occurred widespread in Italy in the recent past as well as in the last centuries. Seismic and volcanic phenomena have affected sporadically large areas, while rainfall-induced landslides, floods and snow avalanches have frequently hit sites spread all over the territory. Structural mitigation approaches are inapplicable throughout the entire territory at risk and might be planned only for areas relevant from a socio-economic point of view.

Hence, to manage natural risks, an increasing effort is being put in the development of non-structural approaches, which rely on prompt forecasting or recognizing of the catastrophic phenomena, so to early spread the alarm throughout the exposed areas (early warning) and temporarily eliminate or, at least, reduce the exposure of people, preventing or limiting victims.

Early Warning Systems (EWS) are among the priorities adopted by the United Nations, International Strategy for Disaster Reduction (ISDR) (UN-ISDR, 2005). They indeed present undeniable advantages, among which are their fast, simple and low-cost implementation, and environmental friendliness. Focusing on water-related hazards, significant examples of operational early warning systems are currently found in the field of floods, landslides, snow avalanches, earth fill failures. A recent review of EWS operating in Europe for water-related hazards can be found in Alfieri et al. (2012).

As it will be described in detail hereinafter, the architecture of an EWS is strictly related to the time needed for the deployment of the mitigation measures, compared to the time of evolution of the hazardous event. In this respect, EWS for floods present quite different features if they are established along large or small rivers. In the first case, rainfall measurements or predictions are supplemented with river stage measurements in upstream sections (e.g. Rabuffetti and Barbero, 2005), and flood routing models can be run in cascade of hydrological models (e.g. Cranston and Tavendale, 2012). The lead time of prediction, which depends on the length of the river and on the extension of its catchment, can extend up to several days or weeks. In the case of small streams, the time lapse between rainfall and peak discharge may be so short that weather now castings needed for the warning to be launched in due time (e.g. Alfieri and Thielen, 2015; de Saint-Aubin et al., 2016).

So far, most of the EWS dealing with rainfall-induced landslides are based on rainfall measurements, sometimes supported by weather forecasts (e.g. Keefer et al., 1987; Ponziani et al., 2012), rarely integrated with monitoring of some soil variables (e.g. Ortigao and Justi, 2004; Chleborad et al., 2008; Baum and Godt, 2010). Rainfalls are interpreted often merely statistically, with an empirical quantification of rainfall



1 thresholds for landslide initiation (e.g. Guzzetti et al., 2007, 2008; Tiranti and Rabuffetti,
 2 2010, Sirangelo and Versace, 1996; Sirangelo and Braca, 2004). In rare cases, physically
 3 based approaches are adopted for the interpretation of the effects of rainfall history.
 4 The few examples of inclusion of slope infiltration and stability modelling in the
 5 assessment of the safety conditions are mostly still at a prototypal stage (e.g. Schmidt
 6 et al., 2008; Ponziani et al., 2012; Eichenberger et al., 2013; Pumo et al., 2016).

7 EWS operating for snow avalanches monitor snow accumulation and the melting
 8 processes, with the former basing essentially on interpreting precipitation and air
 9 temperature records, and the latter on air (or snow) temperature (e.g. Liu et al., 2009).

10 Even in the field of man-made systems, early warning is assuming a prominent role in
 11 the assessment of the risk associated with failure. For instance, in the field of earth
 12 dams, with regard to all possible collapse mechanisms, i.e. slope instability and internal
 13 erosion phenomena, or even earthquake-induced effects, risk mitigation is de-facto
 14 based on early warning systems (e.g., Pagano & Sica, 2013; Ma and Chi, 2016). The wide
 15 monitoring system commonly installed to characterize time-by-time the behavior of
 16 these structures, carried out essentially in terms of displacements, pore water pressure,
 17 seepage flows, accelerations, is pointed towards a continuous checking of dam safety
 18 conditions, aimed at evacuating downstream settlements in case of predicted collapse.

19 In the different fields above considered, literature indicates that common elements,
 20 which typically characterize an early warning system, are:

- 21 1. *a field monitoring system*, recording physical quantities related to the phenomenon
 22 in hand, and transmitting them to a collection-elaboration center; measured
 23 variables may conveniently be distinguished into two categories: *cause variables*,
 24 leading to the initiation of the phenomenon; *effect variables* that, affected by the
 25 formers, characterize the phenomenon itself at the triggering stage or during its
 26 evolution, allowing also to recognize its intensity;
- 27 2. *an interpretative model*, formalizing mathematically the relationships linking cause
 28 and effect variables, allowing to catch the evolution stage of the phenomenon and
 29 assess system safety conditions;
- 30 3. *thresholds* for the variables related to safety conditions of the system; these
 31 thresholds correspond to different alert levels, with the highest one activating the
 32 spread of the alarm message, aimed at eliminating people exposure;
- 33 4. different *actions* related to each alert level defined at 3.

34 Research efforts aimed at the development and implementation of effective EWS
 35 should concern, above all, the definition and calibration of the interpretative model
 36 (Michoud et al., 2013). It should be as accurate as possible and, at the same time,



capable of rapidly carrying out the turning of the monitored quantities into the assessment of system safety conditions. In many applications, dealing with rapidly evolving phenomena, a real-time working system is in fact required, in order to maximize the lead time available for people exposure elimination.

This paper analyses the main features characterizing predictive models working in early warning systems, by discussing their aims, the evolution stage of the phenomenon where they should be incardinated, and their architecture, regardless of the specific application field. Then, examples of application to EWS for rainfall-induced landslides are presented. In particular, the proposed examples refer to the case of cohesionless shallow covers, chosen as they pose challenges that are quite representative of a number of other natural phenomena that might be mitigated by means of early warning systems.

2. Prediction uncertainty and the minimization of the costs of missing and false alarms of an EWS

Whatever the predictive model adopted, it will never be capable of providing certainty about the occurrence of a destructive phenomenon. A model yields variables systematically affected by a given uncertainty degree due to the following possible causes:

- incompleteness of information about the physical system supposed to cause catastrophes;
- various error types associated with the measurements provided by the monitoring system;
- unavoidable simplifications of reality introduced in the predictive model;
- randomness of some of the processes involved in the genesis of the catastrophic event.

It is obvious that all the uncertainties of the predicted variables related to the physical system safety affect the assumption of different alert stages. With reference to the last stage, it may occur that the early warning system sends an alarm, but no dangerous phenomena occur (false alarm) or, conversely, that a dangerous phenomenon takes place without any issued alarm (missing alarm). Both false and missing alarms result into costs for the community supplied with the EWS. A lower uncertainty degree in the prediction is required to minimize their number and, consequently, costs during the system operation. Efficiency of the EWS is therefore considered with respect to the system economic performance for the community, rather than to safety performance.



1 In this sense, alarm activation has to account for the uncertainties associated with each
 2 alert threshold and its overcoming, so to minimize false and missing alarms and related
 3 costs.

4 Decisional rules regarding actions associated with each alert threshold should be based
 5 not only on the mere quantification of thresholds themselves, but also on criteria
 6 defining the *sensitivity* of the EWS, intended as setting the activation of the system at
 7 some probability of a given threshold to be exceeded.

8 The most suitable strategy to quantify such probability of threshold exceedance cannot
 9 be generalized. It is in fact strongly affected by the following peculiarities characterizing
 10 the EWS in hand:

- 11 - the uncertainty of the prediction, which may be reduced by increasing the initial
 12 investment (by preliminary acquiring more information about physical system
 13 features, implementing a more reliable monitoring system with higher spatial and
 14 temporal resolution, elaborating a more sophisticated and accurate predictive
 15 model);
- 16 - the costs suffered by the community in case of false alarm, in turn depending also on
 17 the kind of actions planned in case of threshold exceedance;
- 18 - the costs resulting from a missing alarm with catastrophic event occurrence,
 19 depending on both the event (type and intensity) and resilience of the exposed goods
 20 (related to their nature as well as to socio-economic aspects).

21 In setting up the sensitivity of the EWS, it should be taken into account that too many
 22 false alarms would discredit the system, implying that, with the passing of time, the
 23 served community would contribute less in carrying out all the required actions after
 24 alerts. In short, the sensitivity has to be calibrated on the basis of a cost-benefit analysis,
 25 which can be properly carried out only if the uncertainty of model predictions can be
 26 estimated after an adequate period of monitoring of the physical system

27

28 **3. Evolution stages of a natural hazard: when should the model do the prediction?**

29 In order to generalize a typical architecture for the predictive model, it comes useful to
 30 account for a conventional sequence of stages describing the evolution of a natural
 31 phenomenon resulting into a catastrophe (Figure 1):

- 32 (a) the predisposing stage: the cause variables are subject to such changes to induce
 33 significant modifications of effect variables; the EWS crosses the intermediate
 34 alert thresholds, approaching the alarm threshold;



- 1 (b) the triggering and propagation stage: the failure occurs locally (triggering time)
- 2 and propagates from point to point throughout the physical system up to get the
- 3 physical system itself entirely involved;
- 4 (c) the paroxysmal stage: the physical system collapses and the kinematic of the
- 5 system goes on, eventually hitting the exposed goods.

6

7 The duration of each stage may greatly vary, depending on both the phenomenon type
 8 and on the features of the physical system involved.

9 In a seismic phenomenon involving structures located at a given site “S”, the
 10 *predisposing stage* (a) is determined by the occurrence of the seismic event at the
 11 epicenter and is indicated by the first arrival of the seismic waves at the seismometers
 12 nearest to the epicenter. The *triggering and propagation stage* (b) is determined by
 13 acceleration values exceeding the threshold for first local damages to structural
 14 elements and is monitored by seismic stations located at “S”; the *paroxysmal stage*(c)
 15 consists of the collapse of parts of the structures. For this specific example, the duration
 16 of the stages (a) and (b) is few tens of seconds, while the duration of the stage (c)
 17 depends on the system considered, spanning from seconds for systems like buildings,
 18 rock slopes, gas conduits etc., until hours or even days for natural earth slopes, dams,
 19 and, in general, systems which collapse is determined by a slow redistribution or
 20 propagation of earthquake induced effects.

21 In a rainfall-induced landslide, the *predisposing stage* (a) is determined by the sequence
 22 of rainfall events increasing pore water pressure and worsening slope stability
 23 conditions. The *triggering and propagation stage* (b) spans from the first local slope
 24 failure until the formation of a slip surface. The *paroxysmal stage* (c) is the sliding of the
 25 mobilized soil mass downhill along the slip surface. In this second example, the duration
 26 of each stage is strongly related to the geomorphology of the specific slope, and may
 27 vary from minutes (e.g., flow slides in slopes covered with shallow coarse grained soils)
 28 to even years (e.g., earth flows in slopes of fine grained soils).

29 In a snow-avalanche, the *predisposing stage* (a) is determined by snow accumulation
 30 and temperature increments; the *triggering and propagation stage* (b) starts when
 31 local failures take place within the snow aggregate and ends with a slip surface
 32 formation. The *paroxysmal stage* (c) starts when the mass slides downhill. In this
 33 example, the duration of stage (a) may be of hours or days, depending on the evolution
 34 of atmospheric variables, the duration of stage (b) results undetectable, and the
 35 paroxysmal stage lasts only few seconds.



1 For the case of an overflow in a river, the *predisposing stage* (a) is a sequence of
 2 precipitation events within the watershed, causing a progressive increase of the water
 3 level along a branch of the river; in this case, the *triggering and propagation stage* (b)
 4 and the *paroxysmal stage* (c) are hardly distinguishable from each other. In fact, both
 5 stages start when the first local overflow takes place, and both develop with the flood
 6 propagating around the river. The stage duration depends on the extension and
 7 geomorphology of the watershed. The entire phenomenon may last tens of minutes
 8 (e.g., flash floods in small streams with relatively small catchment) to several days (e.g.,
 9 large rivers with large hydrographic basin).

10 It is also important to highlight that for most phenomena the triggering event has to be
 11 considered as random and, as such, time and location of its occurrence can be predicted
 12 only with a probabilistic approach. On the other hand, the predisposing stage can be
 13 usually described with physical laws, so that its spatial and temporal evolution can be
 14 predicted deterministically by mathematical models.

15 For instance, the strategies followed for early warning with respect to snow avalanches
 16 (e.g., Bakkeoi, 1987) neglect the detection of any possible triggering cause. These may
 17 be internal to the physical system (related to some peculiar morphologies favoring the
 18 susceptibility to local failures) or external (e.g., a skier path cutting transversally the
 19 snow layer slope or a rock-mass falling onto the layer). The randomness of such kind of
 20 triggering causes make them undetectable and useless for early warning purposes.
 21 However, it should be noted that these causes may become effective only if a
 22 predisposing state takes place in terms of snow layer thickness and temperature. This
 23 leads to define the different alert levels on the basis of these two factors, for which
 24 experimental quantification is easy and reliable. Consequently, the warning does not
 25 deal with exactly identifying when, where and what specific triggering cause might
 26 generate an avalanche.

27 In general, early warning prediction can be carried out during any of the above-defined
 28 evolution stages. The choice of the particular stage should obviously consider that
 29 elapsed times needed to predict the event, spread the alarm and eliminate people
 30 exposure must not exceed the time after which the destructive event occurs. On the
 31 other side, the limited time available in-between prediction and event should indicate
 32 which kind of actions could be reasonably carried out. So, only in some cases it will be
 33 possible to consider the opportunity to evacuate all buildings of an entire neighborhood
 34 or forbid all exposed streets to traffic and people access. In some cases, the small
 35 available time only leaves the opportunity for some short actions, such as the
 36 interruption of dangerous supplied services (gas and electricity) or closure of important
 37 infrastructures highly exposed, such as railways or highways.



1 The first step that has to be followed in the development of the predictive tool is hence
 2 the detailed study of the mechanisms that control the evolution of the phenomenon in
 3 hand, and identify which phenomenon stage is the most suitable for the assessment of
 4 safety conditions. For some problems, the choice necessarily falls into a specific stage,
 5 while for others the choice may be multiple. For instance, the slow kinematic of
 6 landslides in fine grained soils allows to place the predictive tool in any of the above
 7 defined three stages, while the rapid kinematic of rainfall-induced landslides in coarse
 8 grained soils prevents considering the paroxysmal stage.

9

10 **4. The architecture of the predictive model**

11 The second step of the development of the predictive tool is choosing the interpretative
 12 model. Promptness and reliability are mandatory requirements of the prediction. The
 13 promptness is usually obtained by introducing model simplifications, which should
 14 however not imply excessive accuracy losses, because they would increase
 15 uncertainties and, consequently, false and missing alarms. An increase of model
 16 complexity should correspond to a reduction in the observational scale of the
 17 phenomenon. Complex models can only be applied to slope scale problems, while,
 18 increasing the observational scale from local to regional, progressive simplifications
 19 have to be introduced in the model and, consistently, less ambitious goals have to be
 20 set in terms of reliability.

21 The wide variety of applications for EWS makes it difficult to generalize criteria to guide
 22 the choice of the predictive model. It is only possible to refer to some classification
 23 criteria, of aid in clarifying the philosophy of the chosen approach, and what ingredients
 24 it requires for its best implementation.

25 A first classification criterion distinguish between empirical and physically-based
 26 models. Empirical models extract relationships among cause and effect variables from
 27 available monitoring data taken over a prolonged time interval. Once set up the
 28 empirical relationships, they typically do not take into any account the physics
 29 governing the phenomenon. Their reliability essentially depends on the amount,
 30 accuracy and representativeness of the available data-set.

31 On the other hand, physically-based models relate cause and effect variables through
 32 mathematical relationships derived straightforwardly from the physical principles
 33 governing the considered phenomenon. The mathematical description of the model
 34 typically involves the assumption of simplifications that strongly affect the accuracy of
 35 the prediction.



1 These two categories may also be used contextually in setting up predictive tools
2 consisting of physically-based as well as of empirical steps.

3 The second criterion of classification refers essentially to physically-based models, and
4 is strictly related to the need for a rapid prediction. It distinguishes between on-line and
5 out-of-line predictions. The former consist in real-time solution of the model equations,
6 updated continuously over time with changes in boundary conditions indicated by field
7 monitoring. The latter, instead, define simple mathematical equations or abaci relating
8 cause and effect variables, by solving the governing equations preliminarily for a
9 number of possible scenarios in terms of initial and boundary conditions (e.g, Pagano
10 &Sica, 2013). These simple mathematical equations or abaci represent the predictive
11 tools adopted to rapidly interpret the data from field monitoring.

12 Strictly related with the selection of the model is, finally, the design of the monitoring
13 system. It has to be consistent with all the choices made about the previously illustrated
14 points. The considered specific stage of phenomenon evolution, as well as the choice
15 of the predictive model, unequivocally identify the physical variables to be monitored,
16 their location and, finally, the number of measurement points.

17 In the following sections, the different features above highlighted will guide along the
18 illustration of some application cases developed in the field of rainfall-induced flow-like
19 landslides.

20

21 **5. Examples of set up and calibration of the predictive tool for early warning**

22 In Italy the destructive potential of rainfall-induced rapid flowslides and debris flows is
23 sadly known. The significance of the problem in terms of number of events and victims
24 becomes clear by merely referring to the disasters occurred over the last years in
25 Campania (Cascini&Ferlisi, 2003, Calcaterra et al., 2004; Pagano et al., 2010; Santo et
26 al., 2012), Piedmont (Villar Pellice, occurred in 2008), Liguria (Cinque Terre, occurred in
27 2011) and Sicily (Maugeri et al, 2011). The rapid kinematic characterizing the post-
28 failure behavior of these phenomena implies that the setup of an early warning system
29 may not rely on the analysis of the short-lasting paroxysmal stage (Figure 2).

30 Exception is made for early warning systems implemented along some roads or railways
31 where the probability that the sliding mass detaching from a slope directly impacts
32 vehicles is small, while the probability that vehicles crash against previously fallen mass
33 obstructing the road is much higher. In such cases, the alarm might be launched in case
34 of the feared road invaded by fallen masses. Hence, the alarm itself could be based on
35 promptly gathering the occurrence of slope instabilities by carrying out monitoring of



1 displacements, and inhibiting road access in case of recorded movements exceeding
 2 some threshold (Mannara et al., 2009).

3 If the exposed factor is instead likely to be directly impacted by the sliding mass, the
 4 triggering of the instability must be predicted in due advance. The time span required
 5 to eliminate people exposure, typically some hours long, implies that the prediction
 6 should be based on monitoring and interpretation of triggering precursors, carried out
 7 already during the predisposing stage.

8 The phenomena in hand typically involve the mobilization of shallow covers rarely
 9 exceeding 2 meters in thickness, induced by rainfall infiltration and related suction
 10 drop. Further physical variables governing the phenomenon are effect variables
 11 describing soil cover wetting (degree of saturation, water content, water storage).

12 The predictive tool may be built on empirical bases whereas, for the reference
 13 geographical context, historical monitoring data of rainfalls related to their effects are
 14 available. Alternatively, it is possible to adopt physically-based approaches through
 15 which turning at any time rainfall into effect variables related to slope stability
 16 conditions. Different levels of these effect variables or, alternatively, of slope stability
 17 indices derived from them, may be chosen as the alert thresholds of the early warning
 18 system. If the mathematical model of the slope has been properly simplified, it may be
 19 possible to operate “in line” by performing model simulations in few minutes.

20 Recent advances in field monitoring of effect variables, in particular soil suction and/or
 21 water content, nowadays offer an alternative approach to the interpretation of rainfall
 22 effects. Sensors like tensiometers, heat dissipation probes and TDR probes, in principle
 23 could directly deliver all the effect variables needed for the assessment of slope stability
 24 conditions. However, the spatial variability of soil properties likely makes an EWS
 25 relying only on field monitoring of effect variables unreliable. Field data are in fact
 26 always affected by local issues, and so they are poorly representative of the whole
 27 monitored area, unless an extremely rich network of sensors is installed, which in most
 28 cases is unfeasible. Hence, field monitoring should be deployed supplementing, rather
 29 than replacing, the estimation of effect variables by means of a more or less simplified
 30 estimation of rainfall effects.

31 The following application examples refer to single slopes, with extension of few
 32 hectares, located in the Lattari Mountains (Campania, southern Italy) and in the basin
 33 of Stura di Lanzo (Piedmont, northern Italy).

34

35



1 5.1 Empirical approach based on rainfall records

2 The example herein reported refers to the chain of Lattari Mountains and, in particular,
 3 to an area spreading in-between the towns of Pagani and Nocera Inferiore (Campania,
 4 southern Italy). An intensely fractured calcareous bedrock covered by silty volcanic soils
 5 characterizes the geology of the site. Volcanic covers have formed due to pyroclastic
 6 air-fall deposits generated by eruptions, mainly those of the volcanic complex of
 7 Somma-Vesuvius occurred over the last 40000 years. Several rainfall-induced flow-like
 8 landslides have interested these covers over centuries. Numerous phenomena also
 9 occurred in the recent past, usually triggered along slopes with inclination angle
 10 between 30° and 40°.

11 A pluviometer installed in 1950, around 3 Km far from the downslope area, provides a
 12 daily rainfall series spanning over 50 years (Pagano et al., 2010). During this period,
 13 three significant flow-like landslides occurred in 1960, 1972 and 1997. Daily rainfall
 14 heights triggering the three phenomena were 87, 77 and 110 mm, respectively. Figure
 15 3 shows all the observed daily rainfall heights larger than the minimum value followed
 16 by a landslide ($h_{dL} = 77\text{mm}$), plotted in ascending order. It may be noticed that the
 17 condition $h_{ds} > h_{dL}$ was met 39 times, but only twice a landslide was actually triggered.
 18 This low correspondence between daily rainfalls and landslides depends on the
 19 existence of additional influencing factors, related to the conditions of the soil cover at
 20 the onset of triggering rainfall, which are neglected if only daily rainfall height is
 21 considered. Antecedent precipitation, in particular, is supposed to play a crucial role,
 22 as it determines the amount of water stored in the cover and lowering soil suction
 23 significantly, before the crucial suction drop induced by the triggering rainfall.

24 The effects of antecedent precipitations may be taken into account by assuming that,
 25 besides the rainfall directly triggering the event (usually identified with rainfall fallen
 26 during the last day), also rainfall cumulating over a longer antecedent period (h_x) plays
 27 an important role in establishing the predisposing conditions for the triggering of a
 28 landslide. The duration “x” of the antecedent period may be chosen as the one
 29 minimizing the number of events (h_{ds} , h_x) characterized by h_x similar to the antecedent
 30 precipitation, h_{xL} , accumulated before the three observed landslides. The minimization
 31 yielded $x=2$ months. This value for x corresponds to h_{2mL} values for all three landslides
 32 of about 500 mm. Over the reference period only 5 rainfall histories (h_{ds} , h_{2m}) resulted
 33 similar to the three (h_{dL} , h_{2mL}) which were followed by in a landslide. If this double
 34 threshold criterion had been virtually implemented as early warning criterion in the
 35 considered area, it would have produced 5 false alarms over 50 years.

36



1 **5.2 Stochastic approach**

2 Few examples of real-time predictions of the probability of triggering of rainfall-induced
 3 landslides in a small area (i.e. a slope or a small catchment) can be found in the
 4 literature (e.g. Sirangelo and Versace, 1996; Sirangelo and Braca, 2004; Schmidt et al.,
 5 2008; Greco et al., 2013; Capparelli et al., 2013; Manconi and Giordan, 2016; Ozturk et
 6 al., 2016). This is due to the intrinsic difficulty of having available historical data sets of
 7 rain storms and corresponding landslides occurred in a small area, with enough data to
 8 allow reliable estimation of the probability of landslide triggering during extreme (and
 9 thus rare) rainfall events. Usually, only few landslides occur at a site during an
 10 observation period of typically some decades, so that probabilistic landslide initiation
 11 thresholds are mostly defined at regional scale, so to have a rich data set of observed
 12 landslides (e.g. Terlien, 1998; Guzzetti et al., 2007; 2008; Jakob et al., 2012; Ponziani et
 13 al., 2012; Segoni et al., 2015; Iadanza et al., 2016). The use of physically based models
 14 of infiltration and slope stability can help in the prediction of slope response under
 15 conditions different from those actually encountered during the observation period,
 16 thus allowing the definition of site-specific landslide initiation thresholds (e.g. Arnone
 17 et al., 2011; Ruiz-Villanueva et al., 2011; Tarolli et al., 2011; Papa et al., 2013; Peres and
 18 Cancelliere, 2014; Posner and Georgakakos, 2015; Greco and Bogaard, 2016), which can
 19 be useful for carrying out stochastic predictions. However, the application of such
 20 physically based approaches in operational early warning systems still suffers the
 21 involved computational burden, which makes difficult carrying out in real time the
 22 calculations required for landslide probability assessment. Consequently, empirical
 23 models of the relationship between rainfall and slope stability are still preferred for
 24 early warning purposes (Sirangelo and Braca, 2004; Greco et al., 2013; Manconi and
 25 Giordan, 2016; Ozturk et al., 2016).

26 An example of setting up an early warning predictive tool taking into account the
 27 uncertainty of the prediction has been developed by coupling a stochastic predictive
 28 model of precipitations (Giorgio and Greco, 2009) with the empirical model FLAIR
 29 (Sirangelo and Versace, 1996), which yields predictions of the triggering time for
 30 rainfall-induced landslides.

31 The FLAIR model associates landslide triggering conditions with values of a mobility
 32 function $Y(t)$, obtained by a convolution integral of the rainfall history $R(t)$ with a
 33 suitable transfer function $\psi(t)$, which allows to model a wide variety of
 34 geomorphological contexts, taking into account predisposing conditions generated by
 35 antecedent rainfalls (Iiritano et al., 1998; Sirangelo et al., 2003).



1 The choice of the transfer function and calibration of its parameters are carried out
 2 based on the historical rainfalls data records in a way that the $Y(t)$ function may result
 3 as a suitable indicator of slope stability conditions. In particular, parameters are
 4 calibrated so that peaks of $Y(t)$ correspond to historical landslides, so to identify a
 5 threshold Y_{cr} that, if exceeded, indicates landslide occurrence.

6 The FLAIR model is currently implemented as predictive model in early warning systems
 7 provided for different thresholds of attention, alert and alarm, corresponding to a
 8 progressive approach of $Y(t)$ to the Y_{cr} threshold. As an example, for the case of Sarno
 9 (pyroclastic slopes in southern Italy) the three mentioned thresholds were suggested
 10 at values of $0.4Y_{cr}$, $0.6Y_{cr}$ and $0.8Y_{cr}$, respectively.

11 The coupling with a stochastic predictive model of rainfall allows adopting the FLAIR
 12 model as a predictor of the probability of occurrence of future landslides (Capparelli et
 13 al., 2013). In fact, the convolution integral may be separated into two parts, one
 14 deterministic, the other random. The first integral computes the convolution of the
 15 rainfall history $R_{obs}(t)$ until the time at which the prediction is carried out. The second
 16 integral computes the convolution of the rainfall history $R_{pre}(t)$ predicted for the future
 17 time interval t_{pre} , the upper bound of which represents the lead time of the prediction:

$$18 \quad Y(t) = Y_{det} + Y_{pre} = \int_{-\infty}^{t-t_{pre}} \Psi(t-\tau) R_{obs}(\tau) d\tau + \int_{t-t_{pre}}^t \Psi(t-\tau) R_{pre}(\tau) d\tau \quad (1)$$

19 The prediction of Y_{pre} is carried out by evaluating the probability conditioned to the
 20 trend of the rainfall observed before prediction. To this aim, the model DRIP
 21 (Disaggregated Rectangular Intensity Pulse) is adopted (Heneker et al., 2001). It defines,
 22 through an alternating renewal process, the observed alternation of rainfall and dry
 23 periods. This process guarantees, in fact, the stochastic independence of a rainfall event
 24 from the duration of the immediately preceding dry period as well as from the duration
 25 and the total rainfall height of the previous rainstorm. This allows carrying out the
 26 conditioned prediction Y_{pre} by only taking into account the rainfall history observed
 27 during the current event, when the prediction is being carried out.

28 The prediction Y_{pre} is carried out by a non-parametric approach, by selecting within the
 29 historical data set only the N_i rainfall events meeting the following conditions: their
 30 duration was equal or longer than the observed part of the current rainstorm; along a
 31 time interval as long as the lead time, t_{pre} , before the prediction, the mobility function
 32 increased in the same proportion as it occurred during the last observed t_{pre} interval of
 33 the current rainfall event.

34 The rainfall events selected by following this procedure allow computing the expected
 35 value of Y_{pre} and the probability that, at the end of the interval t_{pre} , the condition $Y > Y^*$



occurs, whatever Y^* . Hence, once alert and alarm thresholds of the mobility function are defined, the sensitivity of the early warning system can be adjusted by setting up the probability of threshold exceedance at which the relevant messages are launched (activation probability), so to obtain the best trade-off between false and missing alarms (Greco et al., 2013). Low values of the activation probabilities result in high number of alerts and alarms, and may lead to wrong activations of the system (false alert/alarms). Conversely, a less sensitive system unavoidably increases the number of erroneous non-activations of the system (missing alerts-alarms).

The choice of the more suitable values at which setting the activation probabilities represents an important and crucial feature in the setting of an effective early warning system. As already specified previously, the system sensitivity has to take into account all consequences relating with false and missing alarms. For the alert level, it is usually better to set a high sensitivity, since actions determined by alert activations usually do not imply high costs, nor a significant involvement of the served community. The same, however, cannot be stated for the alarm level, as the procedures resulting from alarm spread usually imply high costs and discomfort for the community. As an example, evacuation of people involve stopping all activities and interruption of all infrastructures and services of public utility.

The described approach has been applied to the slope of Pessinetto, 40 km North-East of Turin. The slope, oriented towards South-West, with inclination angle between 30° and 35° , is part of the watershed of the river Stura di Lanzo. It is constituted by a metamorphic bed-rock intensively fractured, covered by a clayey-silt. Six debris flows of different volumes occurred there, within an area of about 1 km^2 , from November 1962 to October 2000. The thickness of mobilized soils ranged between 1.5 and 2.0 m, with soil volumes ranging between few hundreds to 10000 m^3 .

For the calibration of the stochastic model and of the alert system, the pluviometer data recorded in Lanzo, located 6.5 km east of the slope, were available. In particular, the calibration has been carried out by interpreting the hourly precipitations recorded between 1 January 1956 and 10 September 1991. Subsequent data, from 11 September 1991 to 15 June 2004, have been adopted to validate the predictions.

The critical value for the mobility function, estimated over the calibration period, was $Y_{cr}=168.4 \text{ mm/days}$.

The minimum duration of a dry period in-between two rainfall events has been set equal to 10 hours. By assuming only rainfall events exceeding 5 mm to be significant for early warning purposes, a series of 1102 rainfall events meeting the requirements in terms of stochastic independency was selected within the calibration period. These



1 selected events were characterized by durations between 1 hour and 182 hours and
 2 rainfall heights between 5 mm and 615 mm (Greco et al., 2013).

3 The validation period of the early warning system included 456 rainstorms with rainfall
 4 heights exceeding 5 mm.

5 The EWS has been implemented through the definition of two different operational
 6 levels: an alert level and an alarm level. The alert triggers as soon as the mobility
 7 function is predicted to approach the value of $Y_a = 0.75Y_{cr}$ with a probability higher than
 8 a predefined threshold P_1 . The alarm is spread when the probability that Y exceeds the
 9 critical value Y_{cr} is higher than a second threshold P_2 . Predictions are updated with a
 10 hourly frequency and refer to a time interval from 1 to 6 hour later than the prediction
 11 time.

12 Two examples of the potentiality of the predictions of the probability of exceeding the
 13 two defined thresholds are given for two rainfall events occurred during the validation
 14 period, both followed by landslides. In particular, the reported predictions were carried
 15 out with lead times of up to 5 hours.

16 The first event occurred between 22 and 25 September 1993, and Y_a and Y_{cr} were
 17 overtaken 54 and 58 hours after the beginning of the rain, respectively. A landslide was
 18 triggered after 60 hours. In the second example, a rainfall event occurred between the
 19 12 and 15 October 2000, Y_a was passed 39 hours after the beginning of the rain storm,
 20 Y_{cr} after 45 hours, and the landslide occurred after 46 hours.

21 The effectiveness of the stochastic approach for early warning is shown in figures 4 and
 22 5. The graphs give the probability of exceeding the alert and alarm thresholds in the
 23 following five hours, predicted in real time. During the two considered rainfall events,
 24 the system predicted high values of the probability of exceeding both thresholds several
 25 hours in advance. In particular, assuming the activation probabilities $P_1 = P_2 = 0.3$, in both
 26 cases (25 September 1993, figure 4; 14 October 2000, figure 5) the alert would have
 27 been issued about 9 hours before the landslide, while the alarm would have been
 28 launched already 6 hours earlier than the triggering time.

29 Hence, by properly setting P_1 and P_2 the EWS would have been capable to launch, in
 30 both cases, the alert and alarm messages several hours before the actual landslide
 31 triggering. Tables 1 and 2 show the influence of different choices for P_1 and P_2 on the
 32 performance of the EWS, evaluated in terms of total numbers of missing and false alerts
 33 and alarms during the entire validation period. It looks clear how the sensitivity of the
 34 early warning system depends on the chosen activation probability: higher probabilities
 35 correspond to larger numbers of missing alarms, and smaller numbers of false alarms.



1 The optimal choice of P_1 and P_2 should be identified by comparing the costs deriving
 2 from false and missing alerts and alarms, with the benefits of the true alarms. As already
 3 pointed out in the previous sections, such a cost-benefit analysis is of course peculiar
 4 of the particular considered case.

5 The capability of spreading the alert some hours earlier than the triggering time is a
 6 non-trivial feature of the system, when it is implemented to mitigate risks from
 7 phenomena characterized by a very rapid evolution, such as debris flows and other
 8 types of fast landslides, as well as flash floods. In these cases, effective measures to
 9 prevent damages and victims may be successfully implemented only if the alarm is
 10 spread sufficiently earlier than the triggering time of the phenomenon.

11

12 **5.3 Physically based approach**

13 In the town of Nocera Inferiore a second pluviometer, installed in 1997, recorded hourly
 14 rainfalls near the slope where on 4 March 2005 the sadly famous landslide of Nocera
 15 Inferiore was triggered (Figure 6). The slope was tilted at 40° and covered with a 2
 16 meters thick layer of silty volcanic soils. Rainfall records are adopted in this example to
 17 validate a physically based approach (Pagano et al., 2010), suitable to take into account
 18 a number of known influencing factors (triggering event, antecedent precipitation,
 19 instantaneous rainfall intensity, evolution of potential infiltration)(Pagano et al., 2008;
 20 Rianna et al., 2014a).

21 The modelling of the boundary value problem has been simplified as much as possible,
 22 but without determining excessive loss in prediction reliability. Only some factors,
 23 considered of minor importance for the problem in hand, were disregarded, according
 24 to Pagano et al. (2010). In particular, a one-dimensional infiltration problem through an
 25 unsaturated rigid medium was set through Richards equations, solved by the FEM code
 26 SEEP/W (GEOSLOPE 2004).

27 Hourly rainfall records were adopted to quantify boundary fluxes at the uppermost
 28 boundary, while at the lowermost boundary two different limit boundary conditions
 29 were assumed (Reder et al., 2017) to account for the possible effects exerted by the
 30 fractured bedrock on the silty volcanic cover: a seepage surface condition, which
 31 simulates the capillary barrier effect in the hypothesis that fractures are empty; a flux
 32 regulated by the unit gradient, which instead approaches the case of fractures filled
 33 with the same material as that constituting the cover. The hydraulic properties of the
 34 soil, i.e. water retention curve and hydraulic conductivity function, were obtained by
 35 means of laboratory tests (Nicotera& Papa, 2007) as well as by coupled measurements



1 of soil matric suction (Jetfill tensiometers) and volumetric water content (TDR) carried
 2 out in a lysimeter (Rianna et al., 2014b).

3 Results yielded by the analyses (Reder et al., 2017) in terms of suction evolution refer
 4 to the hydrological year 2004-2005 (Figure 7), which includes the landslide event. They
 5 clearly show how the predictions indicates a singularity at the triggering time, consisting
 6 in a drop of suction throughout the cover below 3kPa for both boundary condition-
 7 types assumed at the bottom. Analyses conducted for the whole historical series of
 8 recorded rainfalls, covering a time interval of 10 years including the landslide (Pagano
 9 et al., 2010), indicate that the same singularity is yielded by the prediction only once
 10 more. Hence, if this singularity (suction below 3 kPa throughout the cover) had been
 11 adopted as an alarm criterion, the number of false alarms would have resulted
 12 significantly low. Furthermore, the short time required to update the prediction (few
 13 minutes) is consistent with the requirement of promptness of an early warning system
 14 and allows carrying out “in line” predictions.

15

16 **6. CONCLUSIONS**

17 The paper summarizes the essential elements of early warning systems, implemented
 18 for a real time and continuous check of safety conditions with regard to catastrophic
 19 natural phenomena, in order to accomplish a mitigation of the associated risk. In case
 20 of prediction of a paroxysmal phenomenon, the system should start a procedure
 21 leading to the prompt activation of measures for the protection of exposed goods and
 22 people. In particular, the paper highlights the need for detailed knowledge of how the
 23 different stages of the phenomenon develop over time and, in general, of the factors
 24 affecting each stage. Both these requirements are crucial, in order to establish at which
 25 stage the early warning prediction should be implemented to maximize its
 26 effectiveness.

27 With reference to two different phenomena, namely flow-like landslide and earth
 28 flows, both characterized by rapid evolution, the paper describes, by means of three
 29 examples, some alternative approaches to the development of the predictive tool and
 30 to its implementation in an EWS.

31

32

33

34



1 References

- 2 Alfieri L., Salamon P., Pappenberger F., Wetterhall F., Thielen J.: Operational early
 3 warning systems for water-related hazards in Europe. *Environmental Science & Policy*,
 4 21, 35–49, <http://dx.doi.org/10.1016/j.envsci.2012.01.008>, 2012
- 5 Alfieri L., Thielen J.: A European precipitation index for extreme rain-storm and flash
 6 flood early warning. *Meteorological Applications*, 22: 3–13,
 7 <http://dx.doi.org/10.1002/met.1328>, 2015
- 8 Arnone E., Noto L.V., Lepore C., Bras R.L.: Physically-based and distributed approach to
 9 analyze rainfall-triggered landslides at watershed scale, *Geomorphology*, 133, 121–131,
 10 <http://dx.doi.org/10.1016/j.geomorph.2011.03.019>, 2011
- 11 BAKKEHOI S.: Snow avalanche prediction using a probabilistic method. *Avalanche*
 12 *Formation, Movement and Effects*, Proceedings of the Davos Symposium, September
 13 1986, IAHS Publ. 162, 1986
- 14 Baum R.L., Godt J.W.: Early warning of rainfall-induced shallow landslides and debris
 15 flows in the USA, *Landslides*, 7(3), 259–272, [http://dx.doi.org/10.1007/s10346-009-](http://dx.doi.org/10.1007/s10346-009-0177-0)
 16 [0177-0](http://dx.doi.org/10.1007/s10346-009-0177-0), 2010
- 17 Calcaterra D., de Riso R., Evangelista A., et al.: Slope instabilities in the pyroclastic
 18 deposits of the Phlegraean district and the carbonate Apennine (Campania, Italy),
 19 *Proceedings of an International Workshop on Occurrence and Mechanisms of Flows in*
 20 *Natural Slopes and Earthfills held in Sorrento, Italy, 14–16 May 2003*, 61–75, 2004
- 21 Capparelli G., Giorgio M., Greco R.: Shallow Landslides Risk Mitigation by Early Warning:
 22 The Sarno Case, Margottini et al (eds), *Landslide Science and Practice*, Springer-Verlag,
 23 Berlin, 6, 767–772, <http://dx.doi.org/10.1007/978-3-642-31319-698>, 2013
- 24 Capparelli G., Versace P.: FLAIR and SUSHI: two mathematical models for early warning
 25 of landslides induced by rainfall, *Landslides*, 8(1), 67–79,
 26 <http://dx.doi.org/10.1007/s10346-010-0228-6>, 2011
- 27 Cascini L., Ferlisi S.: Occurrence and consequences of flowslides: a case study,
 28 *Proceedings of an International Conference on Fast Slope Movements – Prediction and*
 29 *Prevention for Risk Mitigation held in Napoli, 11–13 May 2003*, 1, 85–92, 2003
- 30 Chleborad A.F., Baum R.L., Godt J.W.: A prototype system for forecasting landslides in
 31 the Seattle, Washington, area, Baum R.L., Godt J.W., Highland L.M. (Eds.), *Engineering*
 32 *geology and landslides of the Seattle, Washington, area*, Geological Society of America
 33 *Reviews in Engineering Geology*, Geological Society of America, Boulder, XX, 103–120,
 34 [http://dx.doi.org/10.1130/2008.4020\(06\)](http://dx.doi.org/10.1130/2008.4020(06)), 2008



- 1 Cranston M.D., Tavendale A.C.W.: Advances in operational flood forecasting in
2 Scotland, Proceedings of the Institution of Civil Engineers - Water Management, 165(2),
3 69-87, <http://doi.org/10.1680/wama.2012.165.2.79>, 2012
- 4 de Saint-Aubin C., Garandeau L., Janet B., Javelle P.: A new French flash flood warning
5 service, Samuels P., Klijn F., Lang M. (Eds.), E3S Web of Conferences, 3rd European
6 Conference on Flood Risk Management, FLOODrisk 2016, Lyon, France, 17-21 October
7 2016, EDP Sciences, Les Ulis, 7, 18-24, <http://doi.org/10.1051/e3sconf/20160718024>,
8 2016
- 9 Eichenberger J., Ferrari A., Laloui L.: Early warning thresholds for partially saturated
10 slopes in volcanic ashes, Computers and Geotechnics, 49, 79-89,
11 <http://dx.doi.org/10.1016/j.compgeo.2012.11.002>, 2013
- 12 GEO-SLOPE: SEEP/W for finite element seepage analysis, GEO-SLOPE International,
13 Calgary, 2004
- 14 Giorgio M., Greco R.: Rainfall height stochastic modelling as a support tool for floods
15 and flowslides earlywarning, Water Engineering for a Sustainable Environment,
16 Proceedings of XXXIII IAHR Congress. Vancouver, International Association of Hydraulic
17 Engineering & Research, August 2009, 6812-6819, 2009
- 18 Greco R., Bogaard T.A.: The influence of non-linear hydraulic behavior of slope soil
19 covers on rainfall intensity-duration thresholds, S. Aversa et al (eds), Landslides and
20 Engineered Slopes. Experience, Theory and Practice, 2, 1021-1025, Taylor and Francis,
21 2016
- 22 Greco R., Giorgio M., Capparelli G., Versace P.: Early warning of rainfall-induced
23 landslides based on empirical mobilityfunction predictor, Engineering Geology, 153, 68-
24 79. <http://dx.doi.org/10.1016/j.enggeo.2012.11.009>, 2013
- 25 Guzzetti F., Peruccacci S., Rossi M., Stark C.P.: Rainfall thresholds for the initiation of
26 landslides in central and southern Europe. Meteorology and Atmospheric Physics, 98,
27 239-267, <http://dx.doi.org/10.1007/s00703-007-0262-7>, 2007
- 28 Guzzetti F., Peruccacci S., Rossi M., Stark C.P.: The rainfall intensity-duration control of
29 shallow landslides and debris flows: an update, Landslides, 5, 3-17,
30 <http://dx.doi.org/10.1007/s10346-007-0112-1>, 2008
- 31 Heneker T.M., Lambert M.F., Kuczera G.: A point rainfall model for risk-based design.
32 Journal of Hydrology, 247 (1-2), 54-71, [http://dx.doi.org/10.1016/S0022-1694\(01\)00361-4](http://dx.doi.org/10.1016/S0022-1694(01)00361-4),
33 2001



- 1 Iadanza C., Trigila A., Napolitano F.: Identification and characterization of rainfall events
2 responsible for triggering of debris flows and shallow landslides, Journal of Hydrology,
3 541, 230-245, <http://dx.doi.org/10.1016/j.jhydrol.2016.01.018>, 2016
- 4 Iiritano G., Versace P., Sirangelo B.: Real-time estimation of hazard for landslides
5 triggered by rainfall, Environmental Geology, 35(2-3), 175-183,
6 <http://dx.doi.org/10.1007/s002540050303>, 1998
- 7 Jakob M., Owen T., Simpson T.: A regional real-time debris-flow warning system for the
8 District of North Vancouver, Canada, Landslides, 9, 165-178,
9 <http://dx.doi.org/10.1007/s10346-011-0282-8>, 2012
- 10 Keefer D.K., Wilson R.C., Mark R.K., Brabb E.E., Brown W.M., Ellen S.D., Harp E.L.,
11 Wieczorek G.F., Alger C.S., Zarkin R.S.: Real-time landslide warning during heavy rainfall,
12 Science, 238, 921-925, <http://dx.doi.org/10.1126/science.238.4829.921>, 1987
- 13 Liu X., Liu Y., Li L., Ren Y.: Disaster monitoring and early-warning system for snow
14 avalanche along Tianshan highway, IEEE International Geoscience and Remote Sensing
15 Symposium, IGARSS 2009, Cape Town. South Africa; 12-17 July 2009, IEEE Geoscience
16 and Remote Sensing Society, 2, 11634-11637,
17 <http://dx.doi.org/10.1109/IGARSS.2009.5418166>, 2009
- 18 Ma H., Chi F.: Major Technologies for Safe Construction of High Earth-Rockfill Dams,
19 Engineering 2, 498-509, <http://dx.doi.org/10.1016/J.ENG.2016.04.001>, 2016
- 20 Manconi A., Giordan D.: Landslide failure forecast in near-real-time. Geomatics, Natural
21 Hazards and Risk, 7(2), 639-648, <http://dx.doi.org/10.1080/19475705.2014.942388>,
22 2016
- 23 Mannara G., Sarnataro A., Sposito P., Piccolo G., Ciancia N., Infante S.: Rete di sensori
24 accelerometrici MEMS per il monitoraggio in continuo di rilievi franosi in ambito
25 ferroviario, SEF09 Sicurezza ed Esercizio Ferroviario I Convegno Nazionale, Roma 20
26 marzo 2009, 2009 (in Italian)
- 27 Maugeri M., Motta E.: Slope Failure. Effects of Heavy Rainfalls on Slope Behavior: The
28 October 1, 2009 Disaster of Messina (Italy), Iai S. (eds) Geotechnics and Earthquake
29 Geotechnics Towards Global Sustainability, Geotechnical, Geological, and Earthquake
30 Engineering, Springer, Dordrecht, 15, 2011
- 31 Michoud C., Bazin S., Blikra L.H., Derron M.H., Jaboyedoff M.: Experiences from site-
32 specific landslide early warning systems, Natural Hazards and Earth System Sciences,
33 13, 2659-2673, <http://dx.doi.org/10.5194/nhess-13-2659-2013>, 2013



- 1 Ortigao B., Justi M.G. 2004: Rio-Watch: the Rio de Janeiro landslide alarm
2 system. *Geotechnical News*, 22(3), 28–31, 2013
- 3 Nicotera M., Papa R.: Comportamento idraulico e meccanico della serie piroclastica di
4 Monteforte Irpino, Progetto PETIT-OSA Monitoraggio Frane: Contributo alle
5 Conoscenze sulla Franosità in Campania, 272–280. ARACNE, 2007
- 6 Ozturk U., Tarakegn Y.A., Longoni L., Brambilla D., Papini M., Jensen J.: A simplified
7 early-warning system for imminent landslide prediction based on failure index fragility
8 curves developed through numerical analysis, *Geomatics, Natural Hazards and Risk*,
9 7(4), 1406–1425, <http://dx.doi.org/10.1080/19475705.2015.1058863>, 2016
- 10 Pagano L.; Picarelli L.; Rianna G.; Urciuoli G.: A simple numerical procedure for timely
11 prediction of precipitation-induced landslides in unsaturated pyroclastic soils,
12 *Landslides*, 7, 273 – 289, 2010
- 13 Pagano L., Zingariello M.C., Vinale F.: A large physical model to simulate flowslides in
14 pyroclastic soils, *Proc First European Conf on Unsaturated Soils: Advances in Geo-
15 Engineering*, Durham, 205–213, 2008
- 16 Pagano L., Sica S.: Earthquake Early Warning for Earth Dams: Concepts and Objectives.
17 *Natural Hazards*, 66, 303 – 318, <http://dx.doi.org/10.1007/s11069-012-0486-9>, 2013
- 18 Papa M.N., Medina V., Ciervo F., Bateman A.: Derivation of critical rainfall thresholds
19 for shallow landslides as atool for debris flow early warning systems, *Hydrology and
20 Earth System Sciences*, 17, 4095–4107, <http://dx.doi.org/10.5194/hess-17-4095-2013>,
21 2013
- 22 Peres D.J., Cancelliere A.: Derivation and evaluation of landslide-triggering thresholds
23 bya Monte Carlo approach, *Hydrology and Earth System Sciences*, 18, 4913–4931,
24 <http://dx.doi.org/10.5194/hess-18-4913-2014>, 2014
- 25 Ponziani F., Pandolfo C., Stelluti M., Berni N., Brocca L., Moramarco T.: Assessment of
26 rainfall thresholds and soil moisture modeling for operational hydrogeological
27 risk prevention in the Umbria region (central Italy), *Landslides*, 9, 229–237,
28 <http://dx.doi.org/10.1007/s10346-011-0287-3>, 2012
- 29 Posner A.J., Georgakakos K.P.: Soil moisture and precipitation thresholds for real-
30 timelandslide prediction in El Salvador, *Landslides*, 12, 1179–1196,
31 <http://dx.doi.org/10.1007/s10346-015-0618-x>, 2015
- 32 Pumo D., Francipane A., Lo Conti F., Arnone E., Bitonto P., Viola F., La Loggia G., Noto
33 L.V.: The SESAMO early warning system for rainfall-triggered landslides, *Journal of
34 Hydroinformatics*, 18(2), 256–276, <http://dx.doi.org/10.2166/hydro.2015.060>, 2016



- 1 Rabuffetti D., Barbero S.: Operational hydro-meteorological warning and real-time
2 flood forecasting: the Piemonte Region case study, Hydrology and Earth System
3 Sciences, 9, 457-466. <https://doi.org/10.5194/hess-9-457-2005>, 2005
- 4 Reder A., Pagano, L., Picarelli, L., Rianna G.: The role of the lowermost boundary
5 conditions in the hydrological response of shallow sloping covers, Landslides 14, 3, 861-
6 873; <https://doi.org/10.1007/s10346-016-0753-z>, 2017
- 7 Rianna G., Pagano L., Urciuoli G.: Rainfall patterns triggering shallow flowslides in
8 pyroclastic soils, Engineering Geology 174, 22- 35, 2014a
- 9 Rianna G., Pagano L., Urciuoli G.: Investigation of soil-atmosphere interaction in
10 pyroclastic soils, Journal of Hydrology 510, 480-492, 2014b
- 11 Ruiz-Villanueva V., Bodoque J.M., Díez-Herrero A., Calvo C.: Triggering threshold
12 precipitation and soil hydrological characteristics of shallowlandslides in granitic
13 landscapes, Geomorphology, 133, 178-189,
14 <http://dx.doi.org/10.1016/j.geomorph.2011.05.018>, 2011
- 15 Santo A., Di Crescenzo G., Del Prete S., Di Iorio L.: The Ischia island flash flood of
16 November 2009 (Italy): Phenomenon analysis and flood hazard. Physics and Chemistry
17 of the Earth, Parts A/B/C, 3-17, [49](https://doi.org/10.1016/j.pce.2011.12.004), <https://doi.org/10.1016/j.pce.2011.12.004>, 2012
- 18 Schmidt J., Turek G., Clark M.P., Uddstrom M., Dymond J.R.: Probabilistic forecasting of
19 shallow, rainfall-triggered landslides using real-time numerical weather predictions,
20 Natural Hazards and Earth System Sciences, 8: 349–357,
21 <http://dx.doi.org/10.5194/nhess-8-349-2008>, 2008
- 22 Segoni S., Battistini A., Rossi G., Rosi A., Lagomarsino D., Catani F., Moretti S., Casagli
23 N.: Technical Note: An operational landslide early warning system at regional scale
24 based on space–time-variable rainfall thresholds, Natural Hazards and Earth System
25 Sciences, 15, 853–861, <http://dx.doi.org/10.5194/nhess-15-853-2015>, 2015
- 26 Sirangelo B., Braca G.: Identification of hazard conditions for mudflow occurrence by
27 hydrological model. Application of FLAIR model to Sarno warning system, Engineering
28 Geology, 73, 267–276, <http://dx.doi.org/10.1016/j.enggeo.2004.01.008>, 2004
- 29 Sirangelo B., Versace P.: A real time forecasting model for landslides triggered by
30 rainfall, Meccanica, 31(1), 73–85, <http://dx.doi.org/10.1007/BF00444156>, 1996
- 31 Sirangelo B., Versace P., Capparelli G.: Forwarning model for landslides triggered by
32 rainfall based on the analysis of historical data file, Servat E., Najem W., Leduc C.,
33 Shakeel A. (eds.), Hydrology of the Mediterranean and Semiarid Regions, IAHS Publ.,
34 278, 298-304, 2003



- 1 Tarolli P., Borga M., Chang K.T., Chiang S.H.: Modeling shallow landsliding susceptibility
2 by incorporating heavy rainfall statistical properties. *Geomorphology*, 133, 199-211,
3 <http://dx.doi.org/10.1016/j.geomorph.2011.02.033>, 2011
- 4 Terlien M.T.J.: The determination of statistical and deterministic hydrological landslide-
5 triggering thresholds, *Environmental Geology*, 35(2-3), 124-130,
6 <http://dx.doi.org/10.1007/s002540050299>, 1998
- 7 Tiranti D., Rabuffetti D. Estimation of rainfall thresholds triggering shallow landslides
8 for an operational warning system implementation, *Landslides*, 7, 471-481,
9 <http://dx.doi.org/10.1007/s10346-010-0198-8>, 2010
- 10 UN-ISDR (United Nations International Strategy for Disaster Reduction): Hyogo
11 framework for action 2005–2015: building the resilience of nations and communities to
12 disasters, World Conference on Disaster Reduction, Kobe, Japan, January 2005
13 (<http://www.unisdr.org/eng/hfa/docs/Hyogo-framework-for-action-english.pdf>), 2005

d_{pre} [h]	$P_1=0.2$			$P_1=0.25$			$P_1=0.3$		
	N_{1L}	N_{1F}	N_{1M}	N_{1L}	N_{1F}	N_{1M}	N_{1L}	N_{1F}	N_{1M}
2	23	7	2	19	3	2	18	2	2
4	27	11	3	22	7	4	21	6	4
6	31	12	3	25	7	4	22	5	5

Table 1

d_{pre} [h]	$P_2=0.2$			$P_2=0.25$			$P_2=0.3$		
	N_{2L}	N_{2F}	N_{2M}	N_{2L}	N_{2F}	N_{2M}	N_{2L}	N_{2F}	N_{2M}
2	16	4	0	14	2	0	11	1	2
4	22	10	0	17	5	0	15	4	1
6	29	16	1	20	7	1	13	4	5

Table 2

CAPTIONS

Figure 1. Evolution stages of a collapse mechanism

Figure 2. Evolution stages of collapse mechanism in rainfall-induced landslides featured by rapid kinematic



1 Figure 3 - Daily and antecedent-bi-monthly rainfalls recorded at the Nocera Inferiore
 2 site and corresponding to significant events (red circles are associated with landslide
 3 triggering, green circle with rainfall histories similar to those resulting in landslides)

4

5 Figure 4. Stochastic approach to early warning: probability of exceeding alert and alarm
 6 thresholds of the mobility function at the slope of Pessinetto, predicted in real time (the
 7 upper panel reports the observed hyetograph) during the storm of 22.09.1993, when
 8 an earth flow occurred 60 hours after the beginning of the rain.

9

10 Figure 5. Stochastic approach to early warning: probability of exceeding alert and alarm
 11 thresholds of the mobility function at the slope of Pessinetto, predicted in real time (the
 12 upper panel reports the observed hyetograph) during the storm of 12.10.2000, when
 13 an earth flow occurred 46 hours after the beginning of the rain.

14

15 Figure 6. The Nocera Inferiore 2005 landslide area (Pagano et al., 2010, modified)

16 Figure 7. Prediction of suction evolution over the hydrological year of the Nocera
 17 Inferiore 2005 landslide at four different depths and for two different hydraulic
 18 conditions at the lowermost boundary (Reder et al., 2017, modified)

19

20 Table 1. Stochastic approach to early warning: numbers of launched (N_{1L}), false (N_{1F})
 21 and missing (N_{1M}) alerts at the slope of Pessinetto for three different lead times t_{pre} and
 22 three different choices of the probability of alert activation P_1 . For each lead time, the
 23 system carried out 964 predictions between 11 September 1991 and 15 June 2004
 24 (validation period).

25

26 Table 2. Stochastic approach to early warning: numbers of launched (N_{2L}), false (N_{2F})
 27 and missing (N_{2M}) alarms at the slope of Pessinetto for three different lead times t_{pre}
 28 and three different choices of the probability of alarm activation P_2 . For each lead time,
 29 the system carried out 964 predictions between 11 September 1991 and 15 June 2004
 30 (validation period).

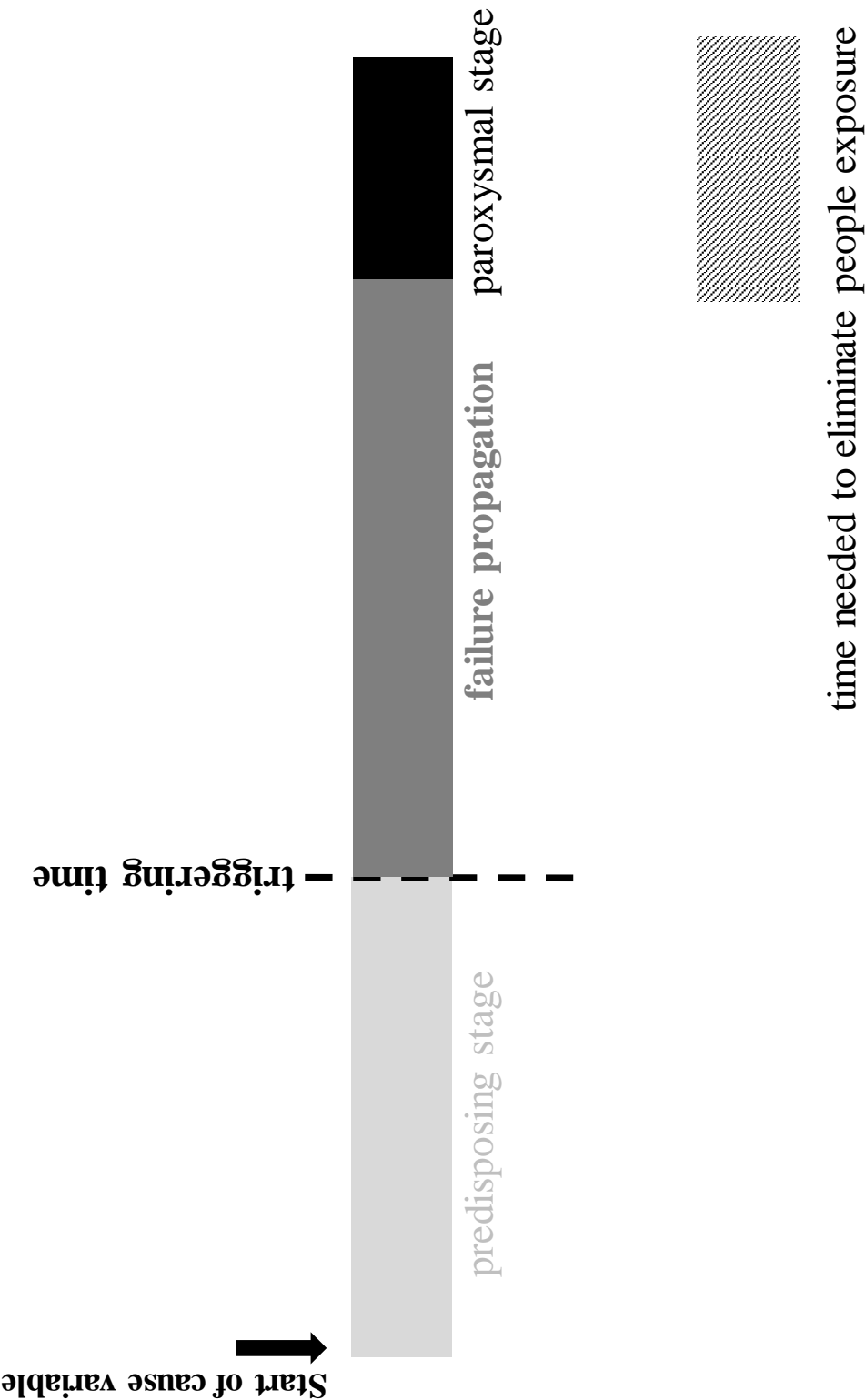


Figure 1

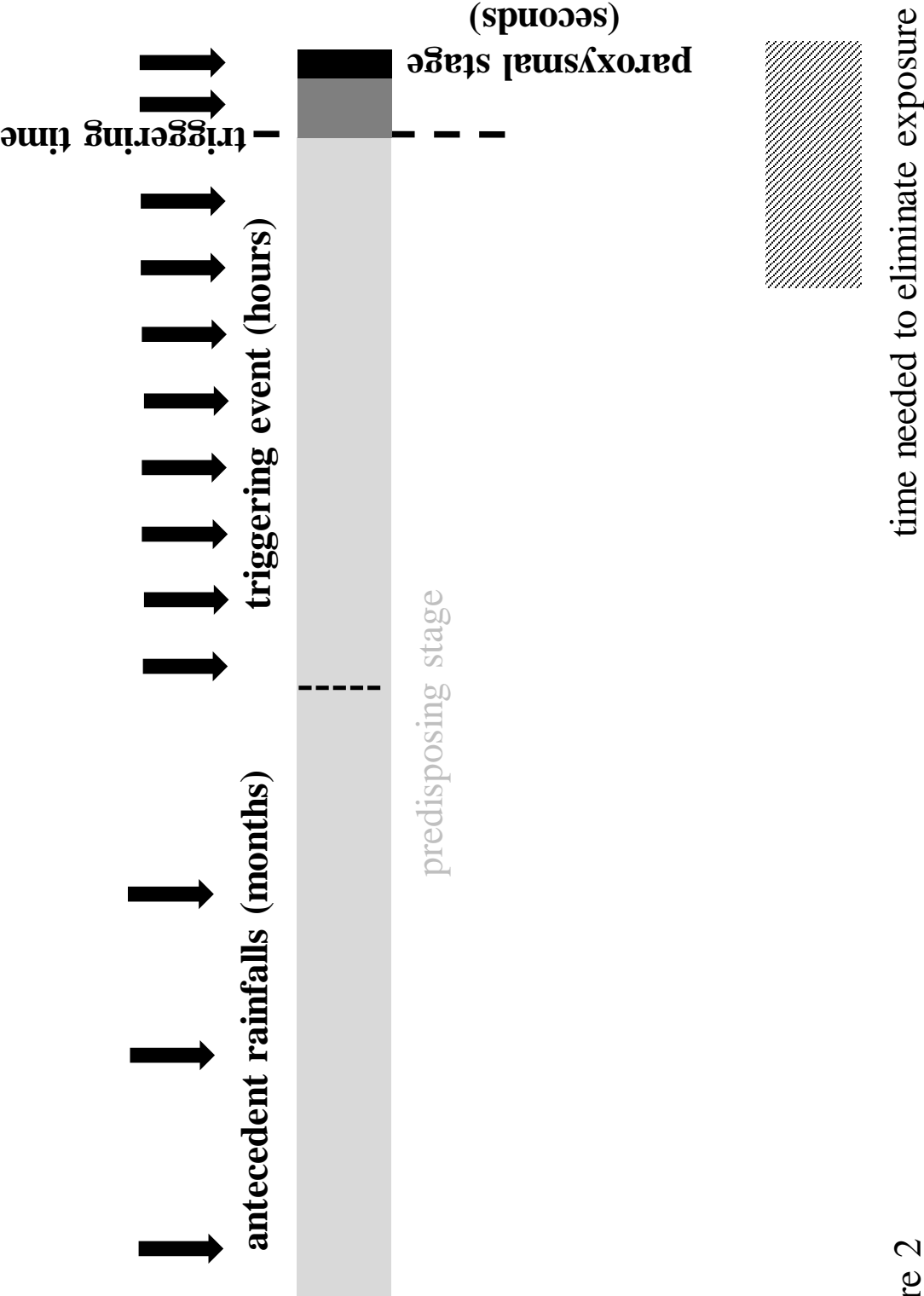


Figure 2

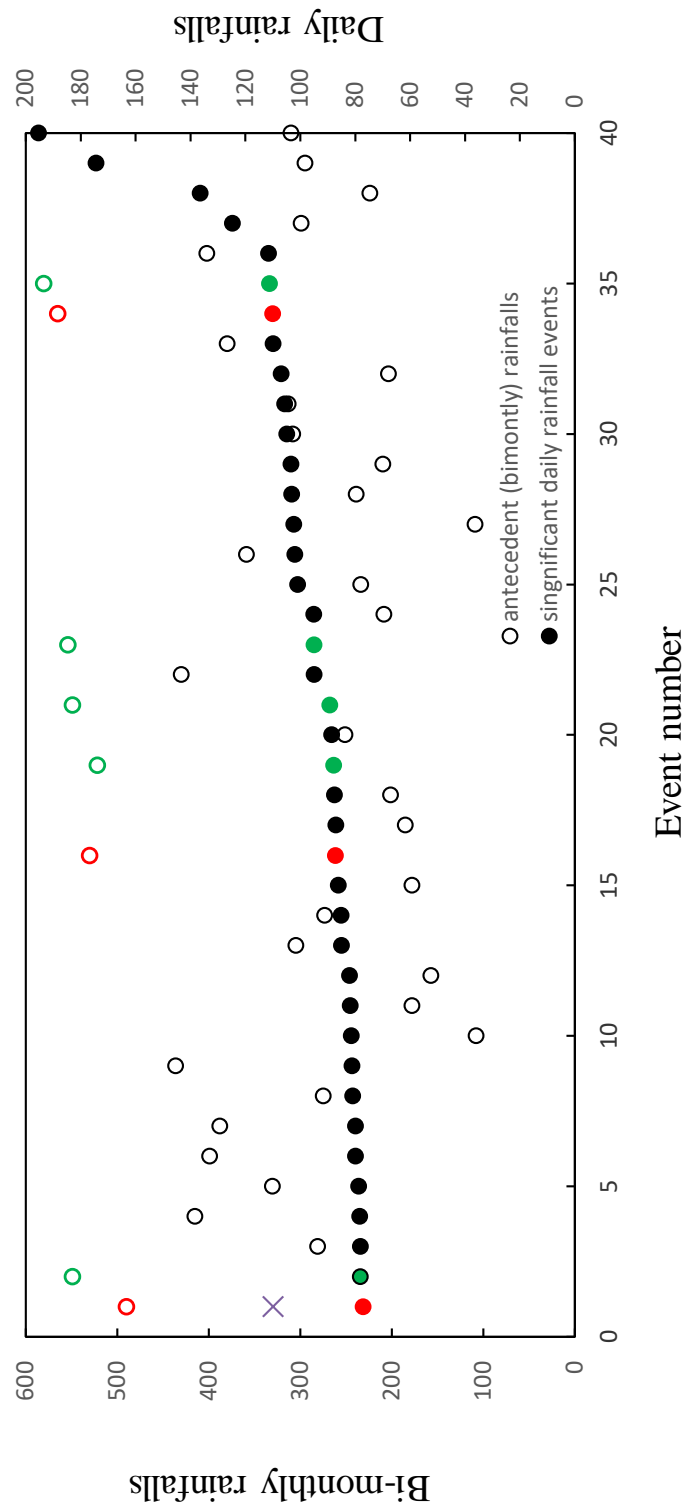


Figure 3

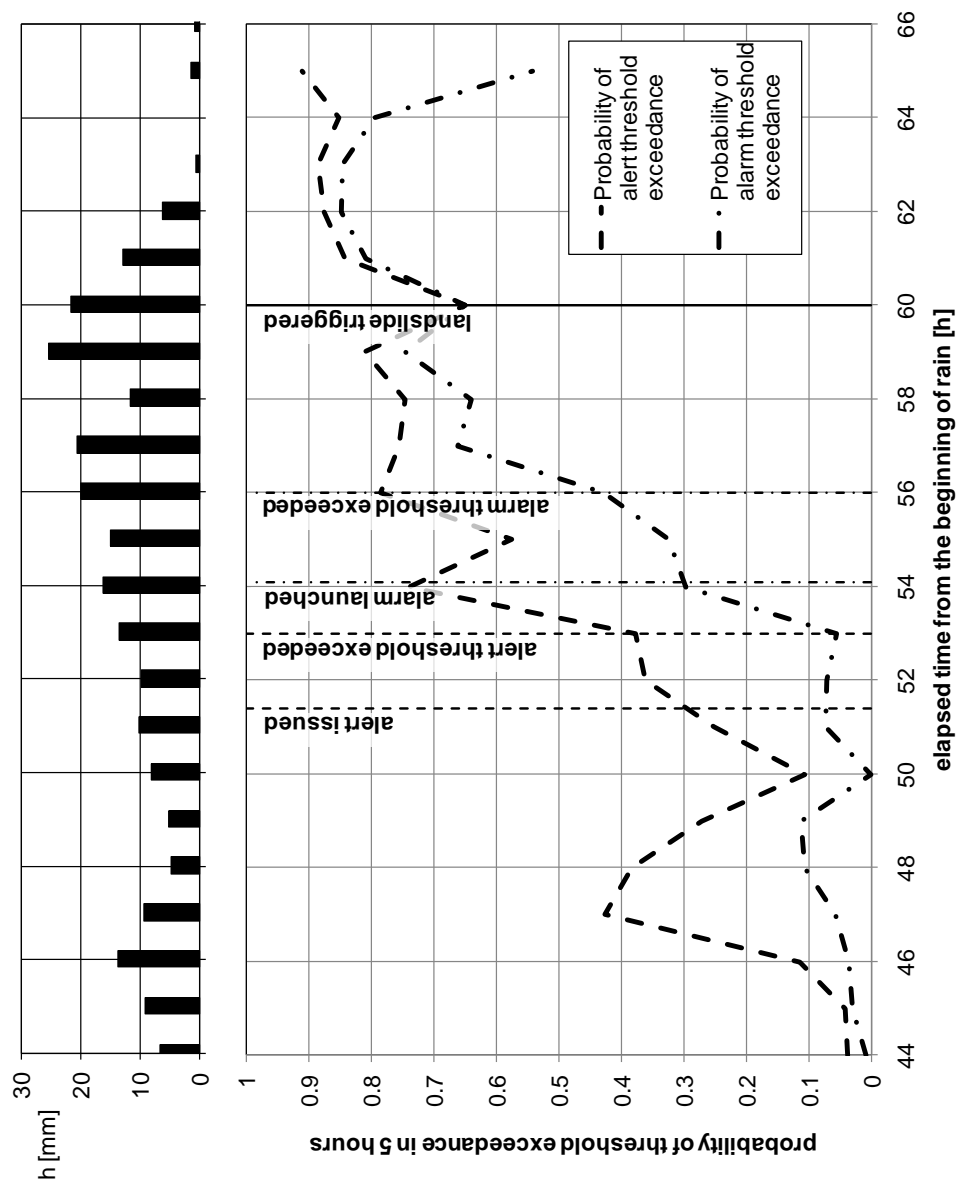


Figure 4

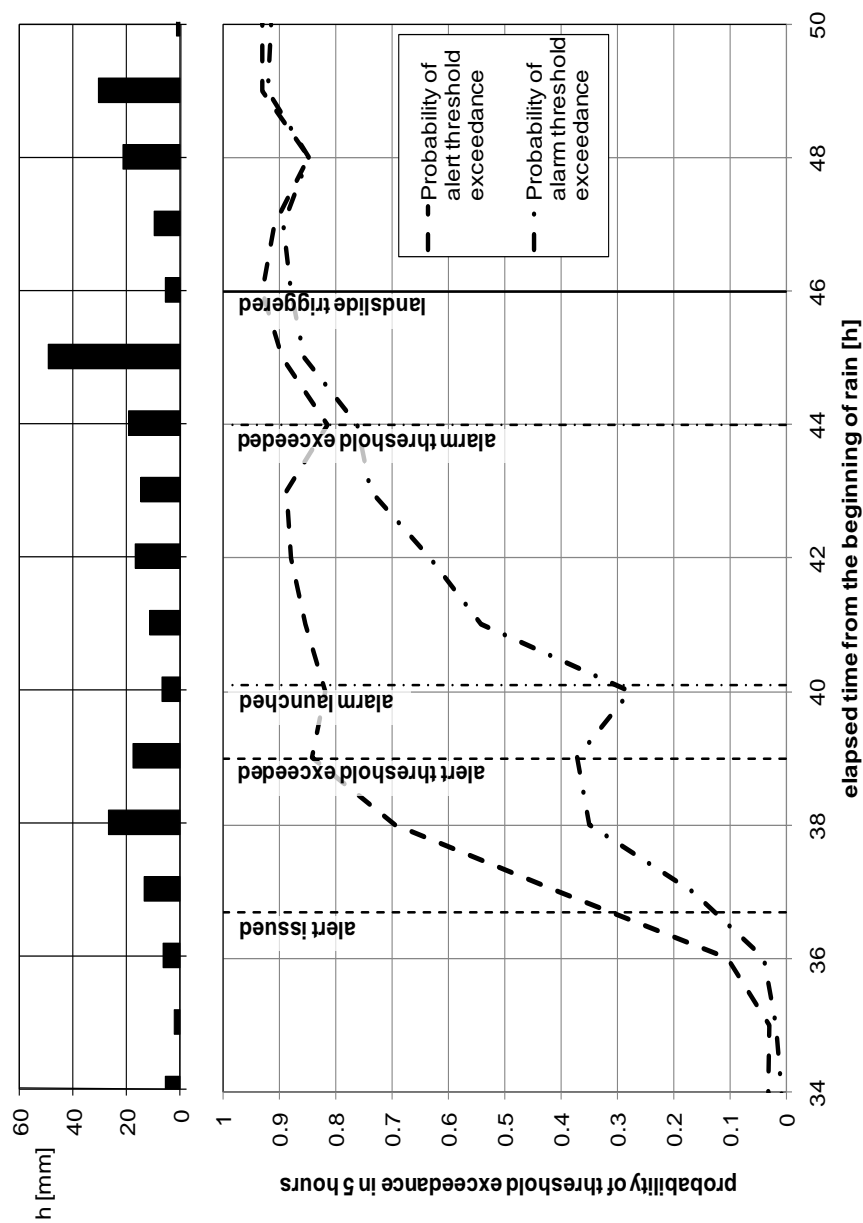


Figure 5

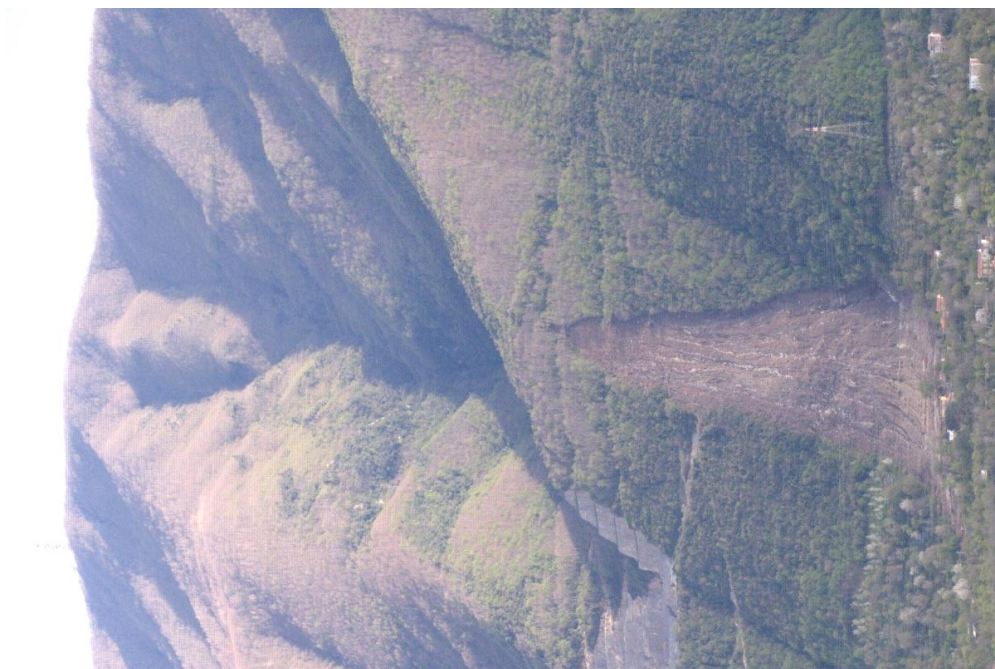


Figure 6

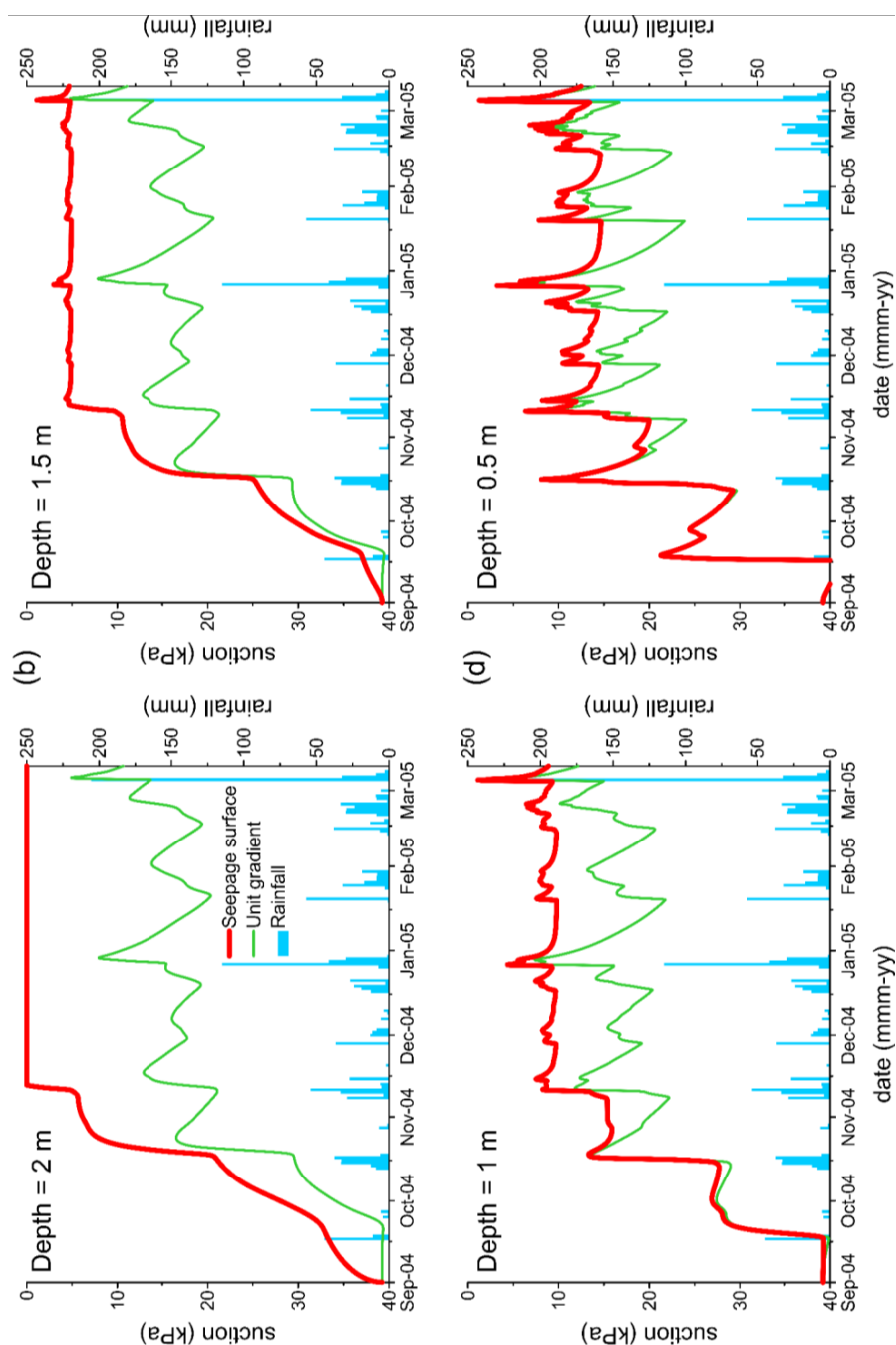


Figure 7